

# Light-Mediated Inhibition of Protein Synthesis

Michael Goard,<sup>2</sup> Girish Aakalu,<sup>2</sup>  
Olesya D. Fedoryak,<sup>1</sup> Carlo Quinonez,<sup>2</sup>  
Jamii St. Julien,<sup>2</sup> Stephen J. Poteet,<sup>1</sup>  
Erin M. Schuman,<sup>2,3,\*</sup> and Timothy M. Dore<sup>1,3,\*</sup>

<sup>1</sup>Department of Chemistry  
University of Georgia

Athens, Georgia 30602

<sup>2</sup>Howard Hughes Medical Institute and

Division of Biology

California Institute of Technology 114-96

Pasadena, California 91125

## Summary

The regulation of protein synthesis is vital for a host of cell biological processes, but investigating roles for protein synthesis have been hindered by the inability to selectively interfere with it. To inhibit protein synthesis with spatial and temporal control, we have developed a photo-releasable anisomycin compound, *N*-([6-bromo-7-hydroxycoumarin-4-yl]methyloxycarbonyl)anisomycin (Bhc-Aniso), that can be removed through exposure to UV light. The area of protein synthesis inhibition can be restricted to a small light-exposed region or, potentially, the volume of two-photon excitation if a pulsed IR laser is the light source. We have tested the compound's effectiveness with an *in vitro* protein-translation system, CHO cells, HEK293 cells, and neurons. The photo-released anisomycin can inhibit protein synthesis in a spatially restricted manner, which will enable the specific inhibition of protein synthesis in subsets of cells with temporal and spatial precision.

## Introduction

Delivering biological effectors to cell and tissue culture samples with temporal and spatial precision is useful for elucidating complex physiological processes. One method for regulating the action of biological effectors utilizes a photolabile-protecting group to render a biological effector inactive ("caged") until it is exposed to a flash of UV light. This cleaves away the protecting group ("uncaging"), resulting in a rapid increase in the effector concentration. A number of photolabile-protecting or "caging" groups have been developed for this purpose [1–4], including *p*-nitrobenzyl (*p*-NB), 4,5-dimethoxy-2-nitrobenzyl (DMNB), and 6-bromo-7-hydroxycoumarin-4-ylmethyl (Bhc) [5], the latter of which is especially useful for controlling the three-dimensional spatial release of biological effectors because of its sensitivity to two-photon excitation [6–11]. Many caged activators of biological function, such as neurotransmitters and second messengers, have been generated

and effectively utilized to study signal transduction, but there are few examples in which a caged antagonist has been used to inhibit a biological process with light [12–18].

The targeting of mRNA and local synthesis of proteins in polarized cells provides specificity to such diverse cell functions as fate specification, body plan formation, axon guidance, and synaptic plasticity. For example, in *Drosophila* the local synthesis of proteins such as oskar [19] or bicoid [20, 21] sets up the initial patterning of the embryo. In neurons, it is likely that local synthesis of proteins in dendrites and axons contribute some of the proteins required for axon outgrowth [22–24] and synaptic plasticity [25–28]. A method for regulating the local inhibition of protein synthesis is desired to better understand the role of local protein synthesis in these and other systems. This paper describes a method for the spatially restricted inhibition of protein synthesis in mammalian cells and neurons with a caged version of the protein-synthesis inhibitor anisomycin, which blocks the peptide-bond-forming reaction in eukaryotic ribosomes [29, 30].

## Results

The caged anisomycins, *p*-NB-Aniso (3a), DMNB-Aniso (3b), and Bhc-Aniso (3c) were synthesized by treating anisomycin with the respective chloroformate of the caging group (Figure 1). The one- and two-photon photolysis properties of each compound were evaluated in order to determine which of the three caged anisomycins is best suited for regulating protein synthesis in neurons. When *p*-NB-Aniso, DMNB-Aniso, and Bhc-Aniso are irradiated with 365 nm light (Figure 1), the reaction progress curves fit to a simple decaying exponential (Figure 2A) with time constants ( $\tau$ ) of 22,173, 187, and 20.9 s, respectively, which correspond to uncaging quantum efficiencies ( $Q_u$ ) of 0.00007, 0.012, and 0.040 mol/ein, respectively. The maximum measured concentration of anisomycin was reached after 100 s of irradiation of Bhc-Aniso. Thus, Bhc-Aniso possesses superior uncaging kinetics when compared to the other compounds, and with an uncaging action cross-section ( $\delta_u$ ) of 0.59 GM, it has sufficient sensitivity to two-photon excitation for biological use (Figure 2B) [5, 11]. Spectroscopic and photochemical (1- and 2-photon) data for the caged anisomycins are summarized in Table 1. All of the caged anisomycin compounds were stable in the dark and behaved similarly under simulated physiological conditions: 98.1% of *p*-NB-Aniso, 97.8% of DMNB-Aniso, and 96.5% of Bhc-Aniso remained after 19 hr at 24°C and pH 7.2 (data not shown). LC/MS monitoring of the dark hydrolysis of Bhc-Aniso revealed that the disappearance of substrate is not a result of hydrolysis of the carbamate linkage but, rather, the loss of the acetate at C3 of anisomycin. No products resulting from carbamate hydrolysis were observed during the time course of the experiment (190 hr).

The ability of the caged anisomycin compounds to

\*Correspondence: schumane@caltech.edu (E.M.S.); tdore@chem.uga.edu (T.M.D.)

<sup>3</sup>These authors contributed equally to this work.

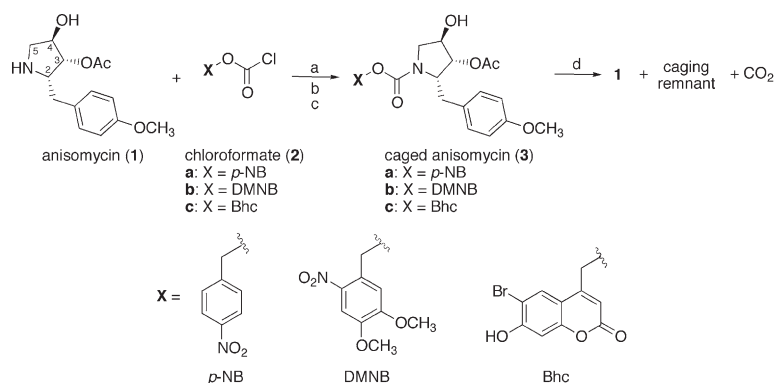


Figure 1. Synthesis and Photochemical Reaction of Caged Anisomycins

Reagents and conditions: (a) Na<sub>2</sub>CO<sub>3</sub>, THF, room temperature (rt), 2 hr, 58%; (b) Na<sub>2</sub>CO<sub>3</sub>, THF, rt, 2 hr, 67%; (c) Na<sub>2</sub>CO<sub>3</sub>, H<sub>2</sub>O, THF, rt, 1 hr, 35%; (d) hv (365 or 740 nm), KMOPS buffer (pH 7.2).

inhibit protein synthesis was then assessed with an *in vitro* translation assay. Bhc- and DMNB-caged anisomycins were activated by exposure to 280–390 nm light for 0.5–10 s. After UV exposure, the compounds were

added to *in vitro* translation reactions at a final concentration of 40 μM (Figures 3A and 3B). The potency of the uncaged compounds in inhibiting protein synthesis was compared to unmodified anisomycin (40 μM). DMNB-Aniso demonstrated a significant inhibition of protein synthesis after 10 s of UV exposure but little inhibition after 2 s of exposure (Figure 3A, lanes 1 and 3). The Bhc-Aniso was able to completely inhibit protein synthesis after as little as 2 s of exposure (Figure 3A, lanes 2 and 4). Both Bhc- and DMNB-Aniso compounds were stable and showed no inhibition of synthesis after 45 min of exposure to ambient light when compared to the vehicle control (Figure 3A, lanes 6–8). Because Bhc-Aniso possessed equal stability and greater uncaging efficiency than the DMNB-Aniso, it was chosen as the compound to use for the local inhibition experiments. Further characterization of the Bhc-Aniso, carried out with irradiation at 365 ± 10 nm, indicated that complete inhibition of protein synthesis could be achieved after 1.4 s of exposure or less (Figure 3B). Note that *p*-NB-Aniso was also able to inhibit protein synthesis after UV exposure, but the required time of exposure, 5 min, and concentration, 400 μM, were prohibitively high (data not shown).

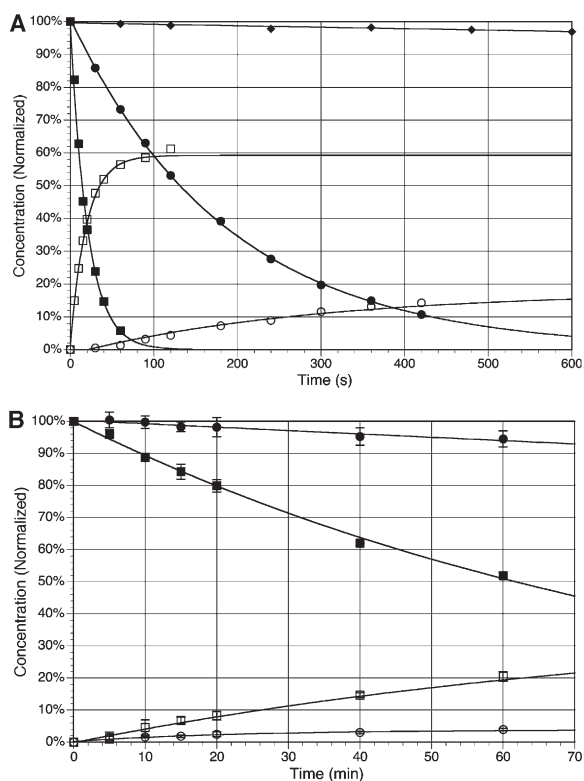


Figure 2. Photolytic Characterization of Caged Anisomycins

(A) Typical one-photon photolysis kinetics of caged anisomycin at 365 nm. Bhc-Aniso (■) was photolyzed to produce anisomycin (□); τ, 20.9 s; R<sup>2</sup>, 0.998. DMNB-Anisomycin (●) was also photolyzed to produce anisomycin (○); τ, 187 s; R<sup>2</sup>, 1.000. *p*-NB-Aniso (◆) did not produce any measurable amount of anisomycin during the time course of photolysis; τ, 22,173 s; R<sup>2</sup>, 0.890.

(B) Time course of two-photon photolysis of DMNB- and Bhc-Aniso. Bhc-Aniso (■) was photolyzed with a mode-locked and fs-pulsed Ti:sapphire laser (740 nm) to produce anisomycin (□); τ, 89.3 min; R<sup>2</sup>, 0.996. DMNB-Aniso (□) was similarly photolyzed to produce anisomycin (○); τ, 917 min, R<sup>2</sup>, 0.943. Error bars represent the standard deviation from at least three measurements.

We determined the effects of UV light on cell viability in order to ascertain tolerable levels of UV exposure. To accomplish this, we exposed cultured hippocampal neurons to UV light of variable duration and then conducted propidium iodide labeling. We found that neurons tolerated a continuous UV-light exposure of up to 1 min (Figures 3C and 3D). Exposure times of 2.5 min or greater led to significant neuronal death; thus, in subsequent experiments, the total UV exposure experienced by cells was always less than 1 min.

To visualize protein-synthesis inhibition dynamically in intact cells, we used a GFP reporter [31] and monitored fluorescence levels in Chinese hamster ovary (CHO) cells before and after local uncaging of Bhc-Aniso. In regions of a culture dish in which the Bhc-Aniso was uncaged by two 500-ms pulses (500-ms interpulse interval) of ~365 nm light every ten minutes, there was a significant reduction in cellular fluorescence over the course of 2 hr (Figures 4A and 4D). In regions of the same dish in which there was no UV-light exposure (and, therefore, no uncaged Bhc-Aniso), the fluorescence levels of cells increased because of new GFP synthesis (Figures 4A and 4D). Thus, we were able

Table 1. Summary of Spectroscopic and Photolytic Characteristics of Caged Anisomycins

Compound	$\lambda_{max}$ (nm)	$\epsilon$ ( $M^{-1} cm^{-1}$ )	$Q_U$ (mol/ein) <sup>a</sup>	$\delta_U$ (GM) <sup>b</sup>
<i>p</i> -NB-Aniso (3a)	274	9,400	$0.007 \pm 0.003 \times 10^{-2}$	—
DMNB-Aniso (3b)	350	6,200	$1.2 \pm 0.1 \times 10^{-2}$	$0.048 \pm 0.003$
Bhc-Aniso (3c)	373	14,500	$4.0 \pm 0.4 \times 10^{-2}$	$0.59 \pm 0.05$

<sup>a</sup>One-photon quantum efficiency for uncaging at 365 nm. Uncertainty is the standard deviation from at least three experiments.

<sup>b</sup>Two-photon uncaging action cross-section at 740 nm (GM,  $10^{-50} cm^4 s/photon$ ). Uncertainty is the standard deviation from at least three experiments.

to locally inhibit synthesis in cells in one region of the culture dish while maintaining uninterrupted protein synthesis in other cells in the same dish.

There is a concern that UV exposure itself may bleach the GFP signal and thereby simulate the predicted effects of protein synthesis inhibition in the cells. We found that this was not the case with our UV-exposure protocol. Cells expressing GFP and exposed to UV (in the absence of Bhc-Aniso) showed a steady increase in GFP fluorescence that was statistically indistinguishable from the increases in fluorescence demonstrated by unexposed controls (Figures 4B and 4D). Compromised cell health was another concern because UV exposure or any free radicals generated in the uncaging process could damage the cells. We assessed by morphological examination and propidium iodide (PI) staining of the UV-exposed cells. The cells expressing the reporter and exposed to UV irradiation did not exhibit any obvious morphological abnormalities or sequester PI, indicating that cell health was not compromised by our uncaging protocol (Figures 4C and 4D).

We next examined the ability of Bhc-Aniso to inhibit protein synthesis in neurons expressing the GFP reporter. We positioned a fiber optic light source in order to uncage Bhc-Aniso in the neuron (Figure 5A). We then monitored GFP fluorescence levels in the dendrites of control neurons and neurons exposed to the uncaging protocol. In control neurons (Bhc-Aniso was applied in the bath but no UV light was administered; “caged”), there was an increase in GFP fluorescence observed in the dendrites over the 3 hr during which images were

acquired (Figures 5B and 5D). In contrast, neurons exposed to UV light in the presence of Bhc-Aniso did not exhibit an increase in dendritic fluorescence but showed a small decrease in fluorescence over time (Figures 5C and 5D). In control experiments, neurons exposed to UV light in the absence of Bhc-Aniso (“flash”) or neurons exposed to DMSO vehicle exhibited increases in dendritic protein synthesis comparable to those exposed to Bhc-Aniso without UV exposure (Figure 5D). The inhibition of protein synthesis induced by uncaging was indistinguishable from that observed in neurons that were treated with anisomycin (40  $\mu$ M) (Figure 5D). This indicates that our uncaging protocol inhibits protein synthesis with the same efficacy as bath application of an unmodified protein-synthesis inhibitor.

We next addressed the spatial specificity of our uncaging protocol by examining the degree of protein-synthesis inhibition as a function of distance from the uncaged region. Time-lapse imaging of HEK293 cells expressing a GFP reporter were obtained before and during uncaging of Bhc-Aniso. We analyzed the change in fluorescence in cells at increasing distances from the uncaging spot. Cells in the center of the spot exhibited maximal decreases in fluorescence levels that were evident 60 min after the onset of uncaging and persisted for at least 3 hr (Figure 6). These decreases were maximal within 100  $\mu$ m from the center of the uncaging spot (Figure 6C). In contrast, cells outside the uncaging spot showed constant or, in some cases, increasing levels of fluorescence during the experiment (Figure 6C). Propidium iodide exclusion assays indicated that UV exposure did not alter the low background levels of cell

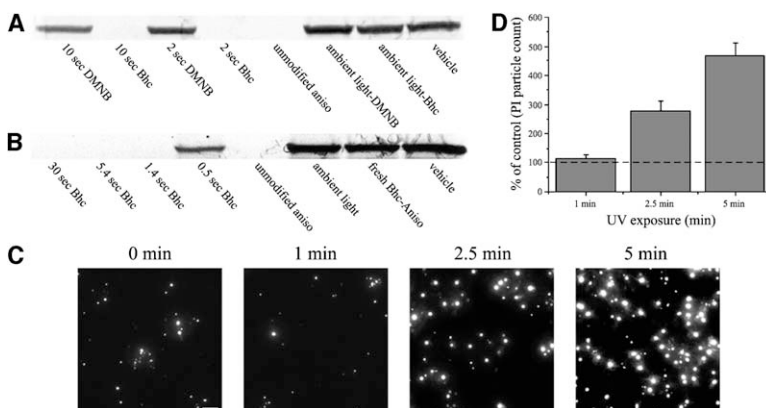


Figure 3. Assessment of the Uncaging Efficiency of Bhc-Aniso and DMNB-Aniso with In Vitro Assays and Characterizing UV Tolerance in Neurons with Propidium Iodide Exclusion Assay

(A and B) Caged anisomycins exposed to various amounts of UV, unmodified anisomycin, caged anisomycin exposed to ambient light, fresh caged anisomycin, and vehicle (DMSO) were added to an in vitro translation reaction. After 1 hr, the [<sup>35</sup>S]-methionine incorporation of these reactions was analyzed by SDS-PAGE. This assay was used to compare the relative uncaging efficiencies of DMNB-Aniso and Bhc-Aniso (A) and to characterize the timescale of Bhc-Aniso uncaging with 365 nm light exposure (B). (C) Cultured neurons exposed to uninter-

rupted UV for 0, 1, 2.5, or 5 min followed by PI treatment. Scale bar, 50  $\mu$ m.

(D) Bar graph showing propidium iodide (PI)-particle count normalized to 0 min exposure controls. N (dishes), 5 for all groups. Error bars represent the standard error of the measurement.

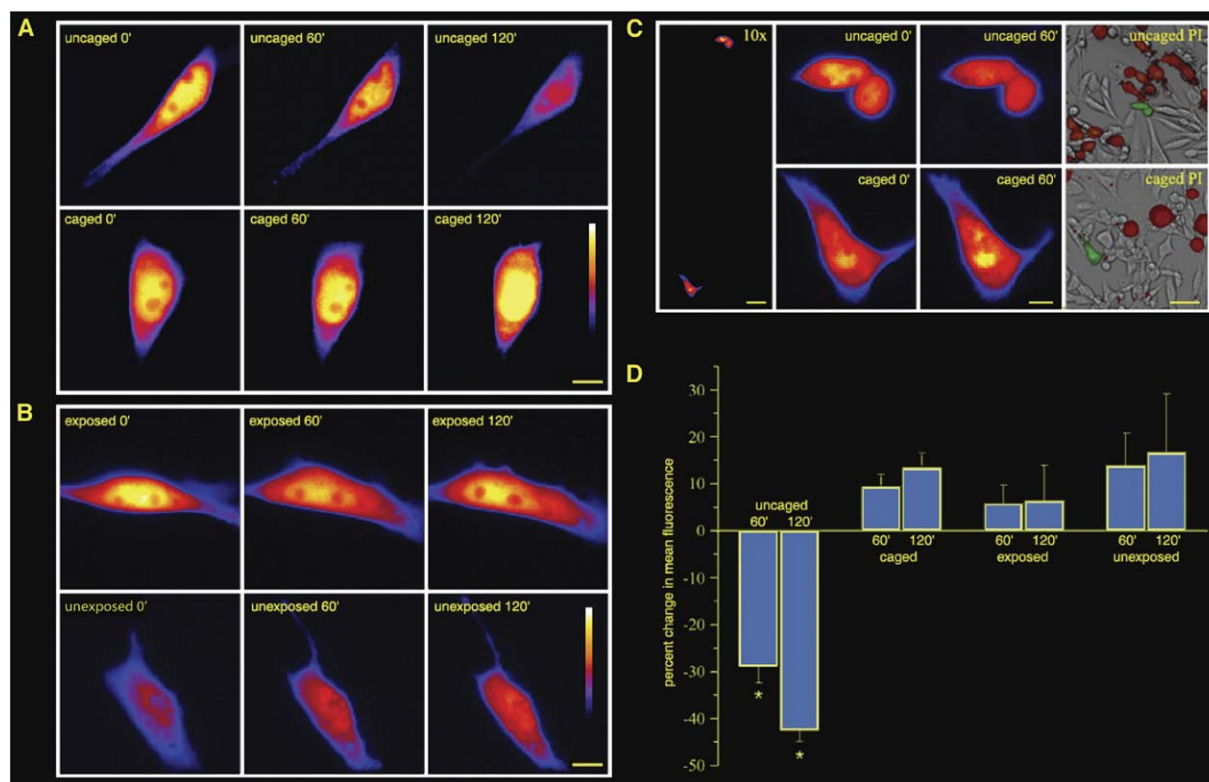


Figure 4. Inhibition of Protein Synthesis in CHO Cells Transfected with GFP Reporter

(A) Uncaging of Bhc-Aniso inhibits GFP synthesis. The top panels show a representative cell that was treated with Bhc-Aniso uncaged by UV exposure (mean fluorescence intensity decreased by 15.8% at 60 min and 42.8% at 120 min). The bottom panels show a cell from the same dish that was treated to Bhc-Anisomycin but had no UV exposure (3.2% increase at 60 min and 20.0% increase at 120 min).

(B) UV exposure alone does not inhibit GFP synthesis. The top panels show a representative cell that was treated with vehicle and UV exposure (12.9% increase at 60 min and 23.4% increase at 120 min). The bottom panels show a cell from the same dish that was outside the UV-exposed region (9.2% at 60 min and 14.3% at 120 min). Scale bar, 10 μm.

(C) Protein synthesis can be locally inhibited by the spatially restricted uncaging of Bhc-Aniso. The leftmost panel shows the relative positions of the UV-exposed (“uncaged”; top) and -unexposed (“caged”; bottom) cells (scale bar, 50 μm). The middle panels show the two cells at 0 and 60 min (24.7% decrease at 60 min for “uncaged” cell, 11.3% increase at 60 min for “caged” cell); scale bar, 10 μm. The right panels show propidium iodide exclusion by each cell at the conclusion of the experiment (green, GFP; red, propidium iodide; scale bar, 50 μm). Lookup table shows scale of fluorescence from no signal (black) to saturated (white).

(D) Summary data for local inhibition experiments in CHO cells. Cells incubated in Bhc-Aniso and exposed to UV (uncaged) displayed a significant decrease over time when compared to cells exposed to Bhc-Aniso without UV (caged), UV alone (exposed), and untreated controls (unexposed) ( $p < 0.01$  for all controls at 60 and 120 min). The caged, exposed, and unexposed groups were not statistically different from each other. N (cells) for each group are as follows: uncaged (6); caged (10); exposed (6); and unexposed (6). Error bars represent the standard error of the measurement.

death observed in HEK293 cells. These experiments indicate that spatially restricted inhibition of the GFP reporter synthesis can be achieved.

## Discussion

We have described a method for the light-controlled inhibition of protein synthesis with a caged protein-synthesis inhibitor, Bhc-Aniso. We have shown that we can significantly inhibit protein synthesis in cells in one region of a culture dish while allowing protein production to go unhindered in other cells (~200–500 μm away) in the same dish. Additionally, this spatially restricted inhibition of protein synthesis had no visible detrimental effect on cell health over the time frame of our experiments (2 hr). Bhc-Aniso is stable in the presence of

ambient light, and it is efficiently photolyzed. The photochemical studies on Bhc-Aniso, DMNB-Aniso, and *p*-NB-Aniso show that the Bhc-caged anisomycin is far more sensitive to single- and two-photon-mediated release of the drug than the DMNB- or the *p*-NB-caged versions. Significant amounts of anisomycin are liberated from Bhc with limited UV exposure, thereby minimizing any toxic effects to cells. Its rapid rate of uncaging may also enable high temporal precision of protein-synthesis inhibition because a high concentration of anisomycin can be rapidly generated.

## Significance

It is now possible to inhibit protein synthesis with both spatial and temporal precision. We have demon-

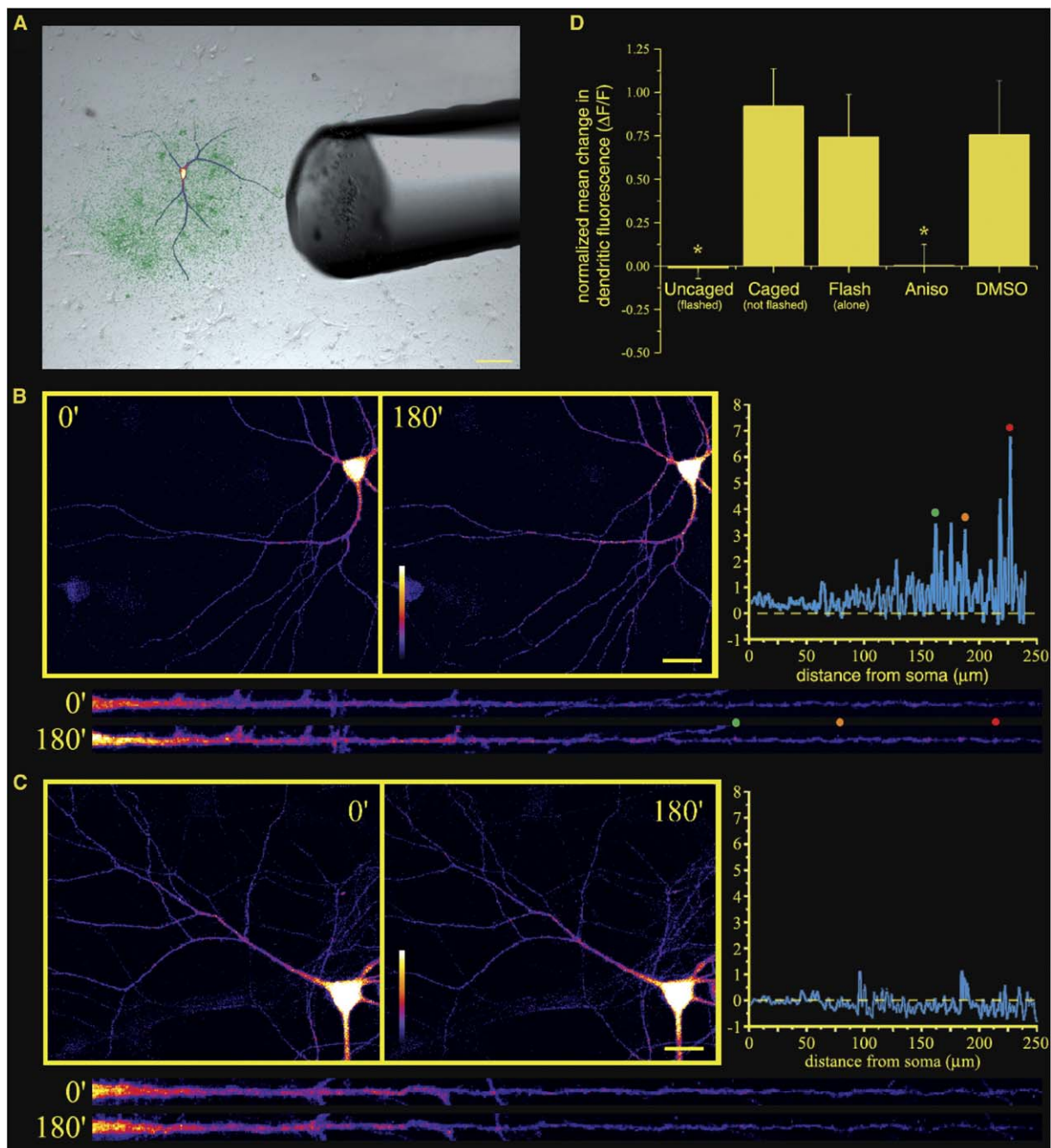


Figure 5. Inhibition of Protein Synthesis in Neurons

(A) Experimental setup for whole-neuron uncaging of Bhc-Aniso. A hippocampal neuron transfected with 5' *m<sub>y</sub>*dGFP3' protein synthesis reporter is shown with 400- $\mu$ m diameter optic fiber positioned to deliver UV light to the neuron.

(B) A representative transfected neuron treated with Bhc-Aniso outside the UV-exposed region ("caged") at 0 (left) to 180 min (middle). Straightened dendrites (bottom) are shown at 0 and 180 min (dendrite length, 250  $\mu$ m), with the change in fluorescence quantified by a  $\Delta F/F$  plot (right). Lookup table ranges from no signal (black) to saturated signal (white); scale bar, 25  $\mu$ m.

(C) A representative neuron from the same dish inside the UV-exposed region ("uncaged") at 0 (left) to 180 min (middle). Straightened dendrites (bottom) are shown at 0 and 180 min (dendrite length, 250  $\mu$ m), with the change in fluorescence quantified by a  $\Delta F/F$  plot (right). Lookup table ranges from no signal (black) to saturated signal (white); scale bar, 25  $\mu$ m.

(D) Neurons treated with Bhc-Aniso and flashed with UV (uncaged) did not increase in fluorescence, similar to cells treated with anisomycin (Aniso). Both of these groups were significantly different ( $p < 0.05$ ) from the three controls: cells treated with Bhc-Aniso but not UV (caged), cells treated with UV in the presence of vehicle (flash), and cells treated only with vehicle (DMSO). The three controls were statistically indistinguishable from each other. N (cells) for each group as follows: uncaged (8); caged (7); flash (6); aniso (9); and DMSO (8). Error bars represent the standard error of the measurement.

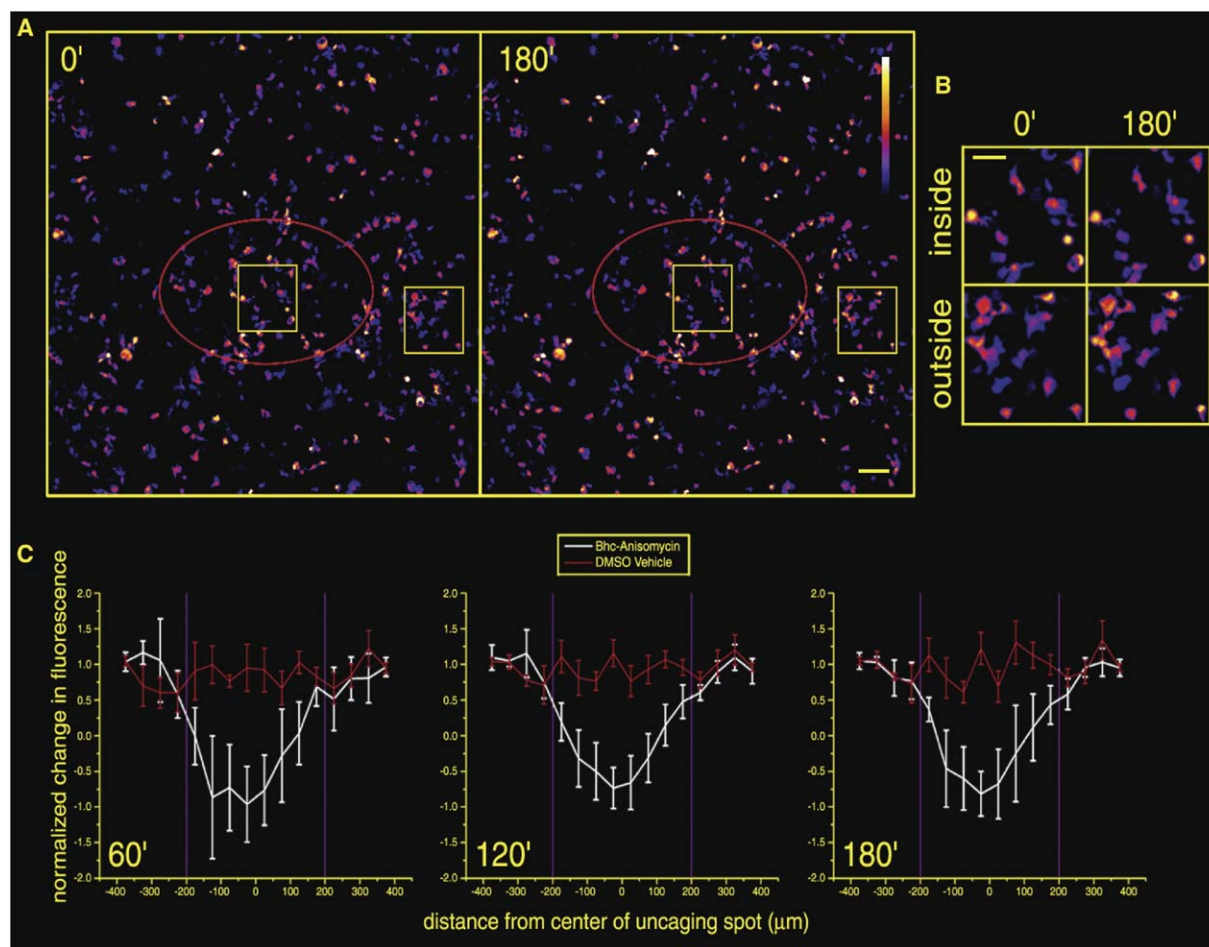


Figure 6. Protein-Synthesis Inhibition Is Spatially Restricted

(A and B) Representative field of HEK293 cells transfected with GFP protein-synthesis reporter at 0 and 180 min. Red oval shows region of UV exposure delivered by 400- $\mu\text{m}$  optic fiber; yellow squares show representative areas inside and outside of the UV-exposure region magnified in (B). Lookup table ranges from no signal (black) to saturated signal (white); scale bar, 250  $\mu\text{m}$ . (B) Magnified regions from (A) inside and outside of the UV-exposure region at 0 and 180 min; scale bar, 50  $\mu\text{m}$ .

(C) Plots showing normalized change in fluorescence versus distance from the center of the UV-exposure region at 60, 120, and 180 min for Bhc-Anisomycin-treated cells (white) and vehicle-treated cells (red). Error bars represent the standard error of the measurement.

strated spatially restricted inhibition with a simple system available to most biological investigators: a fiber optic delivery system with a 100 W mercury arc-lamp light source. These experiments demonstrate that it is feasible to maintain a high concentration of an inhibitor in a restricted region for prolonged periods, opening the door for other compounds to be used in a similar fashion. Nevertheless, the use of more sophisticated light-delivery systems offers the possibility of greater spatial control in more complex systems. Fiber optics can be used to deliver light with a higher spatial specificity than can typically be achieved with a standard microscope objective [32, 33]. Spot sizes of UV illumination as small as 10  $\mu\text{m}$  can be generated by controlling the fiber tip size or by using mirrored micropipettes with small apertures. By using these small spot sizes to activate the caged synthesis inhibitor, one could precisely restrict synthesis in structures as small as a dendritic spine. Fur-

ther spatial regulation of inhibitor action could be achieved if one exploited the large two-photon uncaging action cross-section of Bhc-Aniso, obviating the need to insert a fiber or micropipette into tissue [8–11]. Using this technique would also avoid possible toxicity from long-term UV exposure to cells. This represents a novel method of delivering drugs to biological systems.

#### Experimental Procedures

##### Synthesis of Caged Anisomycins

Anisomycin was purchased from AG Scientific and Sigma. Phosgene was purchased from Fluka as a 20% solution in toluene (1.93 M). 6-Bromo-7-hydroxy-4-hydroxymethyl-coumarin was prepared according to published procedure [5]. Other reagents and solvents were purchased from Aldrich or Fisher and used without further purification.  $^1\text{H}$  NMR and  $^{13}\text{C}$  NMR spectra were recorded on a Varian Mercury 300 MHz, INOVA 500 MHz, or MercuryPlus 400 MHz instrument, as noted. FTIR spectra were recorded on a Bruker Vec-

tor 22 spectrophotometer. UV spectra were recorded on a Cary 300 Bio UV-Visible spectrophotometer (Varian). ESI MS and LC/MS were determined on a Sciex API-1 quadrupole mass spectrometer with an electrospray ionization source. HPLC analysis (analytical and preparative) was performed on a Varian ProStar HPLC system with an autosampler and diode array detector with Microsorb C-18 reverse-phase columns. KMOPS buffer consisted of 100 mM KCl and 10 mM MOPS titrated to pH 7.2 with KOH. Thin-layer and column chromatography were performed on precoated silica gel 60 F<sub>254</sub> plates (EM Science) and 230–400 mesh silica gel 60 (EM Science), respectively.

#### ***N*-(4-Nitrobenzyloxycarbonyl)anisomycin (*p*-NB-Aniso, 3a)**

Anisomycin (1, 90.2 mg, 0.34 mmol), 4-nitrobenzylchloroformate (2a, 75.3 mg, 0.34 mmol), and sodium carbonate (40.7 mg, 0.38 mmol) were stirred in anhydrous THF (4 ml) for 2 hr. The reaction was filtered, and the solvent was removed by rotary evaporation, leaving a yellow oil, which was purified over silica gel with ethyl acetate/toluene (1:1) to yield 87.0 mg (0.197 mmol, 58%) of product 3a. <sup>1</sup>H NMR (300 MHz, CDCl<sub>3</sub>, δ): 7.71 (s, 1H), 7.2–7.0 (m, 3H), 6.77 (d, 2H), 5.52 (m, 2H), 4.88 (m, 1H), 4.46 (m, 1H), 4.02 (m, 1H), 3.95 (s, 6H), 3.76 (s, 3H), 3.6–3.5 (m, 2H), 3.22 (d, 1H), 2.9–2.8 (m, 1H), 2.60 (m, 1H), 2.11 (s, 3H); <sup>13</sup>C NMR (75 MHz, CDCl<sub>3</sub>, δ): 170.8, 158.4, 154.9, 153.6, 148.3, 140.2, 130.4, 129.8, 128.2, 127.6, 114.0, 110.3, 79.1, 78.5, 72.4, 71.8, 64.3, 60.2, 56.6, 55.4, 51.7, 32.9, 21.1; ESI MS, *m/z*: [M + Cl]<sup>-</sup> 479.

#### ***N*-(4,5-Dimethoxy-2-nitrobenzyloxycarbonyl)anisomycin (DMNB-Aniso, 3b)**

Prepared in 67% yield as described for 3a but with chloroformate 2b. <sup>1</sup>H NMR (500 MHz, CDCl<sub>3</sub>, δ): 8.19 (s, 2H), 7.46 (d, 2H), 7.00 (d, 2H), 6.75 (s, 2H), 5.20 (m, 2H), 4.88 (m, 1H), 4.44 (br s, 1H), 4.12–4.04 (m, 1H), 3.74 (s, 3H), 3.58–3.49 (m, 2H), 3.19 (m, 2H), 2.81 (m, 1H), 2.09 (s, 3H); <sup>13</sup>C NMR (125 MHz, CDCl<sub>3</sub>, δ): 170.8, 158.4, 154.8, 147.7, 144.2, 130.3, 129.8, 128.4, 123.9, 114.0, 79.1, 72.2, 66.0, 60.0, 55.3, 51.7, 29.8, 21.0; ESI MS (*m/z*): [M + Na]<sup>+</sup> 527.2.

#### ***N*-([6-Bromo-7-hydroxycoumarin-4-yl)methyloxycarbonyl)anisomycin (Bhc-Aniso, 3c)**

Adapted from lino et al. [34]. Chloroformate 2c was prepared by adding a 20% phosgene solution (1.26 ml, 2.22 mmol) via syringe to a solution of 6-bromo-7-hydroxy-4-hydroxymethylcoumarin (100 mg, 0.37 mmol) in dry THF (4 ml) under nitrogen. The solution was stirred for 1 hr and then purged with nitrogen to concentrate it to approximately half the original volume. In a separate reaction vessel, an aqueous solution of 1.0 M sodium carbonate (0.34 ml) was added to a solution of anisomycin (42 mg, 0.16 mmol) in THF (1 ml). The solution of chloroformate 2c was added dropwise over 10 min to this mixture while stirring and cooling on ice. The reaction mixture was stirred at room temperature for 1 hr. After addition of another solution of chloroformate 2c prepared as described above, the mixture was stirred for 2 hr. The reaction was quenched with 15% citric acid, diluted with chloroform, and extracted with water. The organic layer was dried (MgSO<sub>4</sub>) and evaporated to a residue on the flask wall. The crude product was purified by flash-column chromatography (ethyl acetate/hexane 6:4) to yield 31 mg (0.055 mmol, 35%) of product. <sup>1</sup>H NMR (400 MHz, CDCl<sub>3</sub>, 1.8:1 mixture of conformational isomers, δ): 7.65 and 7.62 (s, 1H), 7.09 and 7.02 (d, 2H), 6.93 (s, 1H), 6.81 (m, 2H), 6.32 and 6.20 (s, 1H), 5.28 (AB q, 2H), 4.96 (m, 1H), 4.48 (br m, 1H), 4.12 and 4.06 (br s, 1H), 3.78 and 3.74 (s, 3H), 3.60 (m, 2H), 3.30 and 2.98 (d, 1H), 2.85 (m, 1H), 2.14 (s, 3H), 2.00 (br, 2H); <sup>1</sup>H NMR (400 MHz, DMSO-*d*<sub>6</sub>, 88°C, δ): 7.89 (s, 1H), 2.75 (dd, *J* = 8.2 Hz, 2H), 6.92 (s, 1H), 6.79 (d, *J* = 8.2 Hz, 2H), 6.19 (s, 1H), 5.30 (AB q, 2H) 4.79 (dd, *J* = 5.1, 10.2 Hz, 1H), 4.28 (m, 1H), 3.95 (dd, *J* = 4.3, 8.6 Hz, 1H), 3.70 (s, 3H), 3.60 (br, 2H), 3.48 (dd, *J* = 5.1, 11.3 Hz, 1H), 3.39 (dd, *J* = 3.1, 10.9 Hz, 1H), 3.50 (br, 1H), 2.75 (dd, *J* = 9.0, 13.7, 1H), 2.04 (s, 3H); <sup>13</sup>C NMR (100 MHz, DMSO-*d*<sub>6</sub>, mixture of conformational isomers, δ): 169.5, 159.6, 157.6, 157.4, 154.0, 153.8, 150.7, 150.1, 129.8, 129.6, 129.5, 128.6, 128.4, 113.6, 110.5, 110.4, 109.5, 108.3, 106.2, 103.1, 77.2, 76.4, 70.1, 69.8, 62.2, 61.6, 59.6, 59.0, 54.8, 51.9, 33.2, 31.8, 20.6; FTIR (neat) 3430, 3188, 3016, 2930, 1750, 1719, 1703, 1688, 1602, 1422, 1219, 656 cm<sup>-1</sup>; ESI MS (*m/z*): MH<sup>+</sup> 562, 564. Samples for characterization,

photochemical analysis, and biological studies were further purified by preparative HPLC (50% CH<sub>3</sub>CN and 50% H<sub>2</sub>O containing 0.1% trifluoroacetic acid).

#### **Measurements of Quantum Efficiencies**

Quantum efficiencies, *Q<sub>u</sub>*, were determined in KMOPS-buffered solutions (3 ml) of the caged anisomycins (100 μM) as previously described [5, 35–38]. Briefly, samples were irradiated with 365 nm light from a mercury lamp (Spectroline SB-100P; Spectronics Corporation, Westbury, NY). The spectral output of the lamp is a distribution across the UV-A wavelengths (310–400 nm) with an intense band at 365 nm. After a period of irradiation, a 20 μl aliquot of the solution was removed for analysis by HPLC with an isocratic mixture of 50% acetonitrile and 50% water containing 0.1% trifluoroacetic acid (flow rate of 1 ml/min). Absorbance was detected at 325 nm (Bhc-Aniso), 345 nm (DMNB-Aniso), 270 nm (*p*-NB-Aniso), and 225 nm (Anisomycin). The progress curves were plotted as simple decaying exponentials. Quantum efficiencies were calculated with  $Q_u = (I\sigma t_{90\%})^{-1}$ , in which *I* is the irradiation intensity in ein · cm<sup>-2</sup> · s<sup>-1</sup>,  $\sigma$  is the decadic extinction coefficient (10<sup>3</sup> ×  $\epsilon$ , the molar extinction coefficient) in cm<sup>2</sup> · mol<sup>-1</sup>, and *t*<sub>90%</sub> is the irradiation time in seconds for 90% conversion to product. The UV intensity of the lamp *I* was measured by using potassium ferrioxalate actinometry [39] in the same setup.

#### **Determination of Dark Hydrolysis Rates of Caged Anisomycins**

Substrates were placed into a KMOPS-buffered solution and stored in the dark at room temperature. HPLC analysis was carried out periodically as described for the quantum efficiency measurements. The identity of the hydrolysis products was determined by LC/MS.

#### **Measurement of Two-Photon Uncaging Cross-Sections**

Cross-sections,  $\delta_u$ , of DMNB-Aniso and Bhc-Aniso were measured as previously described with the HPLC conditions described for the quantum efficiency measurements [5, 37, 38].

#### **In Vitro Translation Experiments**

A given caged anisomycin compound (4 mM in DMSO) was exposed to 280–390 nm or 365 ± 10 nm light (filters from Chroma Technology, Corp., Brattleboro, VT) for the given amount of time. The UV exposure was delivered through a 20× objective (N.A. 0.46) on an Olympus Provis AX 70 microscope with a 100 W mercury arc lamp as the light source. After exposure, the caged compound (or an anisomycin or a vehicle control) was added at a final concentration of 40 μM to an in vitro translation reaction (Promega, Madison, WI) with [<sup>35</sup>S]-methionine incorporation to detect protein synthesis. The level of incorporation after incubation with the inhibitor or control was assessed by SDS-PAGE.

#### **Local Inhibition Experiments in CHO Cells**

CHO cells were maintained and propagated under standard conditions (5% CO<sub>2</sub> in Ham's F12 medium containing 10% fetal bovine serum). Prior to transfection, cells were grown in 35 mm culture dishes or 6-well plates at 95% confluence. Cells were transfected by utilizing Lipofectamine 2000 (Invitrogen, Carlsbad, CA) with a GFP reporter plasmid (pEGFP-C1 [Clontech, Palo Alto, CA]) as described by the protocol provided by Invitrogen.

After 5 hr of transfection, CHO cell growth media was replaced with a HEPES-buffered solution (HBS) [40] (without glycine or picROTOXIN) with 2 mM ascorbic acid and 40 μM Bhc-Anisomycin (or vehicle control). Cells were incubated in this media for 1 hr at room temperature. After incubation, transfected cells were imaged, and one cell (or set of cells) was exposed to 365 ± 10 nm light (Oriol, Stratford, CT) twice for 0.5 s (with a 0.5 s interpulse interval) every 10 min. The UV exposure was delivered through a 40× objective (N.A. 0.80) on an Olympus Provis AX 70 microscope with a 100 W mercury arc lamp as the light source. Subsequent fluorescent images were taken every hour. GFP was excited with a 100 W mercury arc lamp. Single images were taken by using a Hamamatsu digital camera with a 1.5× zoom; excitation filter, 480 ± 40 nm; emission filter, 535 ± 50 nm (Chroma). The exposure time for the images varied depending on the original fluorescence level of the

cells but was kept constant for each dish (both experimental and control cells) throughout the experiment. Cell health was assessed after each local inhibition experiment in CHO cells by propidium iodide (PI) exclusion. Cells were incubated in PI solution (50  $\mu\text{g}/\text{ml}$ ) for 5 min and then washed with HBS. They were subsequently imaged in HBS to assess cell health. The change in GFP fluorescence was quantified by expressing the percentage change in total mean pixel intensity from the 0-min time point to the 60-min or 120-min time point (ImageJ). For comparison of conditions, a one-way ANOVA was performed with the LSD post-hoc test ( $\alpha = 0.05$ ).

#### Local Inhibition Experiments in Neurons

Dissociated hippocampal neuron cultures were prepared from postnatal 2- and 3-day rat pups as described [41]. Neurons were plated at a density of 15,000–45,000 cells/ $\text{cm}^2$  onto poly-L-lysine-coated cell-culture dishes (MatTek). The cultures were maintained and allowed to mature in growth medium (Neurobasal-A supplemented with B27 and Gluta MAX-1) for 14–21 days before use. Dissociated hippocampal neurons were incubated for 30 min in growth medium with the Sindbis virus (construction and production of Sindbis virus containing the 5'  $_{\text{myr}}$ dGFP3' reporter has been previously described) [31], washed with a HEPES-buffered solution (HBS), and placed back in clean growth medium. After the incubation, the growth medium was removed and replaced with HBS containing 5 mM ascorbic acid (pH 7.4) and either caged anisomycin (80  $\mu\text{M}$ ), standard anisomycin (40  $\mu\text{M}$ ), or DMSO (0.05%). Bhc-Aniso (80  $\mu\text{M}$ ) was used so that after the loss of product because of uncaging, the total uncaged anisomycin would be approximately 40  $\mu\text{M}$  and, thus, comparable to the standard anisomycin used in controls (see Figure 1B). The cells were incubated for 1 hr in this medium at room temperature. The dish was then imaged by confocal microscopy (see below), and one cell (or set of cells) was exposed to  $360 \pm 10$  nm light (Oriel) for 45 ms every 11 s (0.095 Hz) for 3 hr, with a total exposure time of 44.2 s for the entire experiment. Flash duration was controlled with a Uniblitz shutter driver (Vincent Associates, Rochester, NY), and the UV exposure was delivered through a 400- $\mu\text{m}$  optic fiber (Rapp OptoElectronic, Hamburg, Germany) with a 100 W mercury arc lamp as the light source. After 3 hr of UV exposure, the 180 min image was taken, and the experiment was terminated. After the end of the experiment, the 365-nm bandpass filter was removed and replaced with a 510-nm bandpass filter. The fiber optic shutter was left open, and an image was acquired in order to visualize the region exposed by UV during the experiment. Greater than 90% of the cell was exposed for all neurons in the “uncaged” and “exposed” conditions. GFP fluorescence was quantified by measuring the mean pixel intensity along the length of the dendrite and with  $\Delta F/F$ , a normalized difference score, as the measure. For  $\Delta F/F$  graphs, five-point adjacent averaging was used for smoothing the plots. For comparison of conditions, a one-way ANOVA was performed with the LSD post-hoc test ( $\alpha = 0.05$ ).

#### Local Inhibition Experiments in HEK293 Cells

HEK293 cells were maintained and propagated under standard conditions (5%  $\text{CO}_2$  in DMEM medium containing 10% fetal bovine serum, 10 units/ml penicillin, and 10  $\mu\text{g}/\text{ml}$  streptomycin). Prior to transfection, cells were grown on poly-L-lysine-coated cell-culture dishes (MatTek). Cells were transfected by utilizing Lipofectamine 2000 (Invitrogen, Carlsbad, CA) with a GFP reporter plasmid (pd1EGFP-N1 [Clontech, Palo Alto, CA]). After 8 hr of transfection, HEK293-cell-growth media was replaced with a HEPES-buffered solution (HBS) [40] (without glycine or picROTOXIN) with 5 mM ascorbic acid and 80  $\mu\text{M}$  Bhc-Anisomycin (or DMSO control). The dish was then imaged by confocal microscopy (see below), and a field of cells was exposed to  $365 \pm 10$  nm light (Oriel) for 45 ms every 11 s (0.095 Hz) for 3 hr, with a total exposure time of 44.2 s for the entire experiment. Flash duration was controlled with a Uniblitz shutter driver (Vincent Associates, Rochester, NY), and the UV exposure was delivered through a 400- $\mu\text{m}$  optic fiber (Rapp OptoElectronic, Hamburg, Germany) with a 100 W mercury arc lamp as the light source. Subsequent fluorescent images were taken every hour for 3 hr at which time the experiment was terminated. After the last image, the 365-nm bandpass filter was removed and re-

placed with a 510-nm bandpass filter in order to image the exposed area during the experiment. The data was analyzed by fitting a  $488 \times 288$  pixel (678  $\mu\text{m} \times 400 \mu\text{m}$ ) ellipse over the uncaging region as determined by the image taken with the 510-nm bandpass filter (because the fiber optic came at an angle, the exposed region at the plane of the cells was an ellipse instead of a circle). Concentric ellipses scaled up or down by 100- $\mu\text{m}$  increments (for both the major axes of the original ellipse) were overlaid on the original fluorescent images with a custom macro in ImageJ. The fluorescence between these ellipses was measured and compared across time points to measure the change in fluorescence as a measure of distance from the center of the uncaging spot. Semiellipses on the top half of the image were analyzed separately from the semiellipses on the bottom half in order to determine whether the inhibition was symmetrical on both sides of the uncaging spot. The measurements on the x axis of the plots in Figure 5C range from the top (outer) semiellipse (–400  $\mu\text{m}$ ) to the bottom (outer) semiellipse (400  $\mu\text{m}$ ).

#### Confocal Microscopy

Confocal images were acquired in 0.5- $\mu\text{m}$  sections; image analysis was conducted on z-compressed image stacks, which contained the entire neuron of interest. GFP was excited at 488 nm, and emitted light was collected between 510–550 nm. Images were acquired with parameters that maximized the dynamic range of pixel intensity for the dendritic signal. The cell-body fluorescence intensity was necessarily, occasionally saturated by using these parameters. Analysis was performed on the major dendrite of neurons exhibiting a pyramidal neuron-like morphology.

#### Acknowledgments

This research was supported by the Howard Hughes Medical Institute, the National Institutes of Health (MH065537, E.M.S.), the University of Georgia Research Foundation, an award from the Research Corporation (T.M.D.), and a University of Georgia Thomas Whitehead Scholarship in Chemistry for summer research (S.J.P.). The authors would like to thank Procter & Gamble for a generous donation of anisomycin and Kenneth A. Miller and Rebekah L. Rogers for technical assistance.

Received: August 3, 2004

Revised: March 23, 2005

Accepted: April 14, 2005

Published: June 24, 2005

#### References

1. Adams, S.R., and Tsien, R.Y. (1993). Controlling cell chemistry with caged compounds. *Annu. Rev. Physiol.* 55, 755–784.
2. Marriott, G. (1998). Controlling cell chemistry with caged compounds. In *Caged Compounds*, Volume 291 (New York: Academic Press).
3. Nerbonne, J.M. (1996). Caged compounds: tools for illuminating neuronal responses and connections. *Curr. Opin. Neurobiol.* 6, 379–386.
4. Pelliccioli, A.P., and Wirz, J. (2002). Photoremovable protecting groups: reaction mechanisms and applications. *Photochem. Photobiol. Sci.* 1, 441–458.
5. Furuta, T., Wang, S.S.H., Dantzker, J.L., Dore, T.M., Bybee, W.J., Callaway, E.M., Denk, W., and Tsien, R.Y. (1999). Brominated 7-hydroxycoumarin-4-ylmethyls: photolabile protecting groups with biologically useful cross-sections for two photon photolysis. *Proc. Natl. Acad. Sci. USA* 96, 1193–1200.
6. Denk, W., Strickler, J.H., and Webb, W.W. (1990). Two-photon laser scanning fluorescence microscopy. *Science* 248, 73–76.
7. Denk, W. (1994). Two-photon scanning photochemical microscopy: mapping ligand-gated ion channel distributions. *Proc. Natl. Acad. Sci. USA* 91, 6629–6633.
8. Williams, R.M., Piston, D.W., and Webb, W.W. (1994). Two-photon molecular excitation provides intrinsic 3-dimensional resolution for laser-based microscopy and microphotochemistry. *FASEB J.* 8, 804–813.

9. König, K. (2000). Multiphoton microscopy in life sciences. *J. Microsc.* *200*, 83–104.
10. Zipfel, W.R., Williams, R.M., and Webb, W.W. (2003). Nonlinear magic: multiphoton microscopy in the biosciences. *Nat. Biotechnol.* *21*, 1369–1377.
11. Dore, T.M. (2005). Multiphoton phototrigger for exploring cell physiology. In *Dynamic Studies in Biology: Phototrigger, Photoswitches, and Caged Biomolecules*, R.S. Givens and M. Goeldner, eds. (Weinheim, Germany: Wiley-VCH), pp. 435–459.
12. Kehayova, P.D., Bokinsky, G.E., Huber, J.D., and Jain, A. (1999). A caged hydrophobic inhibitor of carbonic anhydrase II. *Org. Lett.* *1*, 187–188.
13. Kehayova, P.D., Woodrell, C.D., Dostal, P.J., Chandra, P.P., and Jain, A. (2002). Phototriggered delivery of hydrophobic carbonic anhydrase inhibitors. *Photochem. Photobiol. Sci.* *1*, 774–779.
14. Takaoka, K., Tatsu, Y., Yumoto, N., Nakajima, T., and Shimamoto, K. (2003). Synthesis and photoreactivity of caged blockers for glutamate transporters. *Bioorg. Med. Chem. Lett.* *13*, 965–970.
15. Takaoka, K., Tatsu, Y., Yumoto, N., Nakajima, T., and Shimamoto, K. (2004). Synthesis of carbamate-type caged derivatives of a novel glutamate transporter blocker. *Bioorg. Med. Chem.* *12*, 3687–3694.
16. Shi, Y., and Koh, J.T. (2004). Light-activated transcription and repression by using photocaged SERMs. *ChemBioChem* *5*, 788–796.
17. Montgomery, H.J., Perdicakis, B., Fishlock, D., Lajoie, G.A., Jervis, E., and Guillemette, J.G. (2002). Photo-control of nitric oxide synthase activity using a caged isoform specific inhibitor. *Bioorg. Med. Chem.* *10*, 1919–1927.
18. Perdicakis, B., Montgomery, H.J., Abbott, G.L., Fishlock, D., Lajoie, G.A., Guillemette, J.G., and Jervis, E. (2005). Photocontrol of nitric oxide production in cell culture using a caged isoform selective inhibitor. *Bioorg. Med. Chem.* *13*, 47–57.
19. Ephrussi, A., and Lehmann, R. (1992). Induction of germ cell formation by oskar. *Nature* *358*, 387–392.
20. MacDonald, P.M., and Struhl, G. (1988). Cis-acting sequences responsible for anterior localization of bicoid mRNA in *Drosophila* embryos. *Nature* *336*, 595–598.
21. Berleth, T., Burri, M., Thoma, G., Bopp, D., Richstein, S., Frigerio, G., Noll, M., and Nüsslein-Volhard, C. (1988). The role of localization of bicoid RNA in organizing the anterior pattern of the *Drosophila* embryo. *EMBO J.* *7*, 1749–1756.
22. Campbell, D.S., and Holt, C.E. (2001). Chemotropic responses of retinal growth cones mediated by rapid local protein synthesis and degradation. *Neuron* *32*, 1013–1026.
23. Ming, G.L., Wong, S.T., Henley, J., Yuan, X.B., Song, H.J., Spitzer, N.C., and Poo, M.M. (2002). Adaptation in the chemotactic guidance of nerve growth cones. *Nature* *417*, 411–418.
24. Brittis, P.A., Lu, Q., and Flanagan, J.G. (2002). Axonal protein synthesis provides a mechanism for localized regulation at an intermediate target. *Cell* *110*, 223–235.
25. Casadio, A., Martin, K.C., Giustetto, M., Zhu, H., Chen, M., Bartsch, D., Bailey, C.H., and Kandel, E.R. (1999). A transient, neuron-wide form of CREB-mediated long-term facilitation can be stabilized at specific synapses by local protein synthesis. *Cell* *99*, 221–237.
26. Huber, K.M., Kayser, M.S., and Bear, M.F. (2000). Role for rapid dendritic protein synthesis in hippocampal mGluR-dependent long-term depression. *Science* *288*, 1254–1256.
27. Kang, H., and Schuman, E.M. (1996). A requirement for local protein synthesis in neurotrophin-induced hippocampal synaptic plasticity. *Science* *273*, 1402–1406.
28. Martin, K.C., Casadio, A., Zhu, H., Yaping, E., Rose, J.C., Chen, M., Bailey, C.H., and Kandel, E.R. (1997). Synapse-specific, long-term facilitation of aplysia sensory to motor synapses: a function for local protein synthesis in memory storage. *Cell* *91*, 927–938.
29. Ioannou, M., Coutsogeorgopoulos, C., and Syntetos, D. (1998). Kinetics of inhibition of rabbit reticulocyte peptidyltransferase by anisomycin and sparsomycin. *Mol. Pharmacol.* *53*, 1089–1096.
30. Barbacid, M., and Vazquez, D. (1974). [<sup>3</sup>H]-anisomycin binding to eukaryotic ribosomes. *J. Mol. Biol.* *84*, 603–623.
31. Aakalu, G., Smith, W.B., Nguyen, N., Jiang, C., and Schuman, E.M. (2001). Dynamic visualization of local protein synthesis in hippocampal neurons. *Neuron* *30*, 489–502.
32. Kandler, K., Katz, L.C., and Kauer, J.A. (1998). Focal photolysis of caged glutamate produces long-term depression of hippocampal glutamate receptors. *Nat. Neurosci.* *1*, 119–123.
33. Parpura, V., and Haydon, P.G. (1999). UV photolysis using a micromanipulated optical fiber to deliver UV energy directly to the sample. *J. Neurosci. Meth.* *87*, 25–34.
34. Iino, Y., Ishii, M., Ohsumi, K., and Tsuji, T. October 1995. Anisomycin derivatives and anticancer agents, antifungal agents and antiprotozoan agents containing the same. U.S. patent 5,463,078.
35. Adams, S.R., Kao, J.P.Y., Gryniewicz, G., Minta, A., and Tsien, R.Y. (1988). Biologically useful chelators that release Ca<sup>2+</sup> upon illumination. *J. Am. Chem. Soc.* *110*, 3212–3220.
36. Livingston, R. (1971). Behavior of photochromic systems. In *Photochromism*, G.H. Brown, ed. (New York: Wiley), pp. 13–44.
37. Fedoryak, O.D., and Dore, T.M. (2002). Brominated hydroxyquinoline as a photolabile protecting group with sensitivity to multiphoton excitation. *Org. Lett.* *4*, 3419–3422.
38. Lu, M., Fedoryak, O.D., Moister, B.R., and Dore, T.M. (2003). Bhc-diol as a photolabile protecting group for aldehydes and ketones. *Org. Lett.* *5*, 2119–2122.
39. Hatchard, C.G., and Parker, C.A. (1956). A new sensitive chemical actinometer. II. Potassium ferrioxalate as a standard chemical actinometer. *Proc. R. Acad. London. Ser. A* *235*, 518–536.
40. Malgaroli, A., and Tsien, R.W. (1992). Glutamate-induced long-term potentiation of the frequency of miniature synaptic currents in cultured hippocampal neurons. *Nature* *357*, 134–139.
41. Banker, G., and Goslin, K. (1998). Glutamate-induced long-term potentiation of the frequency of miniature synaptic currents in cultured hippocampal neurons. In *Culturing Nerve Cells* (Cambridge, MA: MIT Press).